

ANALYSING THE TRANSFORMATION OF FOREST LITTER'S ORGANIC MATTER ON DIFFERENT STAGES OF SECONDARY SUCCESSION OF A MIDDLE TAIGA FOREST USING THE FOURIER-TRANSFORM INFRARED SPECTROMETRY¹

© 2025 A. F. Sabrekov^a, * Y. V. Kupriyanova^a, A. A. Koval^a, D. V. Ilyasov^a, M. V. Glagolev^{a, b, c}, and E. D. Lapshina^a

^a Yugra State University, Chekhova st. 16, Khanty-Mansiysk, 628012 Russia

^b Moscow State University, Soil Science Faculty, Leninskie Gory 1 bldg. 12, Moscow, 119991 Russia

^c Institute of Forest Science of the RAS, Sovetskaya st. 21, Uspenskoe, Moscow Oblast, 143030 Russia

*e-mail: sabrekovaf@gmail.com

Received May 20, 2024

Revised October 08, 2024

Accepted November 15, 2024

Abstract. Organic matter decomposition is a key process in the carbon cycle that controls the rate of carbon dioxide emission, carbon accumulation in the soil, and the availability of mineral elements for plants. Changes in the forest stand's composition during secondary succession result in changes in the quality of litter, which affects the rate and depth of its transformation. We analysed how the chemical structure of the L-horizons of litter changes from October to August at different stages of secondary succession in typical forest ecosystems of Western Siberia's middle taiga using IR-Fourier spectrometry and elemental analysis. It turned out that the structure of organic matter in the L-horizons got transformed to the largest degree at intermediate stages of succession (in an aspen forest with a dark coniferous second storey), while at previous (monodominant aspen forests) and subsequent successional stages (mixed and dark coniferous forests), changes were less pronounced. These changes include a decrease in the proportion of relatively easily decomposable components (cellulose and carbohydrates) and accumulation of aromatic compounds and polyesters that are more resistant to decomposition. Aspen forest with the dark coniferous second storey and dark coniferous forest turned out to be the objects with the largest differences in terms of changes in the litter's elemental composition: the ratio of total carbon to nitrogen over the period from October to August increased the least in the former and the most in the latter. This combination of IR Fourier spectrometry and elemental analysis results can be explained by differences in the efficiencies of depolymerisation of nitrogen-containing compounds in litter. In general, the obtained results show that litter transformation during decomposition does not always depend only on its initial quality, even in closely located ecosystems where physical conditions are virtually identical. The functioning of the microbial community may be the cause of these differences in transformation at different stages of succession.

Keywords: forest litter, boreal forest, carbon cycle, nitrogen cycle, Western Siberia

DOI: 10.31857/S00241148250105e9

Management of forest ecosystems has high potential as a technology for absorbing CO₂, a key greenhouse gas for the Earth's atmosphere (Canadell et al., 2021). This is particularly true for disturbed forests, with a more accurate assessment of the potential and identification of the most effective sequestration mechanisms depending on the stage of recovery from disturbance and the region in which the forests are located (Canadell et al., 2021). A number of natural (windthrow, insect pest outbreaks), anthropogenic

(logging, fragmentation, air pollution) and combined (fires) factors lead to disturbance of forest cover (Práválie, 2018; Lukina, 2020), increasing its heterogeneity and forming a mosaic of stands of different ages at different stages of recovery (Accumulation..., 2018). Thus, the study of carbon cycle functioning at different stages of secondary succession is necessary when planning measures to mitigate global climate warming

Decomposition of organic matter occupies an important place in the carbon cycle of natural and anthropogenically modified ecosystems (Kobak, 1988). Dead tissues of primary producers (plants, mosses, algae) accumulate on the soil surface or inside it in the form of ground and root fall, respectively, after which they are transformed by microorganisms with the participation of soil animals. Most of the

¹ The research was carried out as part of the key innovative project of national importance "Key Innovative Project of National Importance, aimed to monitoring the dynamics of climatically active substances in terrestrial ecosystems of the Russian Federation" (Registration number: 123030300031-6).

incoming organic matter is utilized by microorganisms for energy (Kobak, 1988; Wardle et al., 2004), resulting in carbon dioxide emission to the atmosphere. The remainder of the fall is transformed to soil organic matter directly or through incorporation into the biomass of microorganisms (Semenov et al., 2013; Adamczyk, 2021; Angst et al., 2021). Litter decomposition is also important for the nitrogen cycle, especially in nitrogen-poor ecosystems: nitrogen availability to plants here depends on the decomposition of plant debris and, as a consequence, the availability of released nitrogen-containing organic compounds for uptake by roots or mycorrhiza (Zechmeister-Boltenstern et al., 2015; Reuter et al., 2020). Thus, an understanding of the mechanisms and decomposition rates of litter is necessary for informed modeling of the biogeochemical cycle in ecosystems and its response to various influences.

It is well known that the rate of litter decomposition depends on physical (temperature, humidity, availability of oxygen and other electron acceptors) and chemical (pH, presence of inhibitors) conditions, as well as on the quality of the organic matter itself (Cotrufo, del Galdo, 2009; Ge et al., 2013; Ivanova, 2021; Berezin et al., 2023). Also, the physicochemical conditions and quality of the litter affect the decomposition process indirectly through the influence on the diversity and activity of the decomposer organisms — soil zoocenosis and microbocenosis (Cotrufo, del Galdo, 2009; Ge et al., 2013; Berezin et al., 2023). The change of dominant forest species during secondary succession inevitably implies changes in the quality of incoming litter and microbial community composition (Wardle et al., 2004; Fernández-Alonso et al., 2018; Ivanova, 2021). There is no strict definition of quality; high quality litter is considered to decompose faster while low quality litter is considered to decompose slower (Cotrufo, del Galdo, 2009). Indicators of organic matter quality during litter decomposition at different stages of forest secondary succession are most often the ratio of total carbon and nitrogen contents (hereafter C/N), and the proportion of nitrogen (N) in the original organic matter (Ge et al., 2013; Zhang et al., 2013; Fernández-Alonso et al., 2018; Basova et al., 2022). However, these indicators do not always correlate with organic matter decomposition rates because they are based on total contents rather than the fraction available for decomposition (Yang et al., 2022). In addition, they do not allow a detailed analysis of which organic compounds decompose faster and which decompose more slowly.

Another method for investigating the quality of litter during their decomposition in natural ecosystems is Fourier transform infrared spectrometry (FTIR spectrometry) (Heller et al., 2015; Soong et al., 2015; Reuter et al., 2020). This method, on the one hand, is fast and easy to apply and does not require the use of acids and solvents toxic to humans, on the other hand it allows obtaining semi-quantitative information about the main functional groups of an organic substance that determine its chemical properties (Heller et al., 2015). In addition, the

original natural sample is used for analysis by FTIR spectrometry, rather than a sample transformed, for example, in the process of extraction (Heller et al., 2015)

The aim of our work was to compare changes in the quality of organic matter of the L-horizon from the forest floor during decomposition at different stages of secondary succession in a middle taiga forest using FTIR spectrometry. For this purpose, we sampled the L-horizon in ecosystems at different developmental stages (from monodominant aspen to mature dark coniferous forest), just before and immediately after autumn leaf fall. The L-horizon in October contains the maximum amount of fresh litter in the earliest stages of decomposition, and in August contains the maximum amount of litter decomposed during the year. A comparison of these two states of the L-horizon will show how different the process of transformation of the chemical structure of the litter during the different stages of secondary succession is. We hypothesized that, since decomposition of deciduous fall is faster than that of conifers (Ivanova, 2021; Berezin et al., 2023), the change in its chemical structure as decomposition proceeds should become less pronounced at the later stages of succession. We used C/N ratio and total nitrogen content as additional indicators of organic matter quality in L-horizons.

OBJECTS AND METHODOLOGY

The studies were conducted in typical forest ecosystems of the middle taiga of Western Siberia, on the territory of the international field station “Mukhrino”, 25 kilometers southwest of Khanty-Mansiysk (Fig. 1). According to the Keppen-Geiger classification, the climate of the region is subarctic (boreal continental), without dry season and with cold summers (Dfc). The average air temperature for the nearest weather station to the site (Khanty-Mansiysk airport) for the period 1991–2020 in January is -19.1°C , in July $+18.2^{\circ}\text{C}$. The average annual precipitation is 547 mm, 70% of which falls during the growing season from May to October.

Forests in the study area are distributed in well-drained areas along rivers and streams, forming a mosaic of communities depending on how long ago a fire occurred at a particular location, which is the main cause of secondary succession in the middle taiga zone (Kharuk et al., 2021). A few years after the destruction of vegetation, small-leaved forests are formed, which are gradually transformed into mixed and then climax dark coniferous forests. We selected forest plots of 25×25 m with homogeneous vegetation in an upland position with a slope not exceeding 2° (to avoid the influence of moisture differences on litter composition) at different stages of secondary succession typical of the middle taiga of Western Siberia as sample plots (hereafter referred to as PPs). All PPs are located on the first terrace of the Irtysh River, in the valleys of its first-order tributary, the Mukhrinka River, and the Kabanyi Creek flowing into it. The succession series studied by us begins with a middle-aged

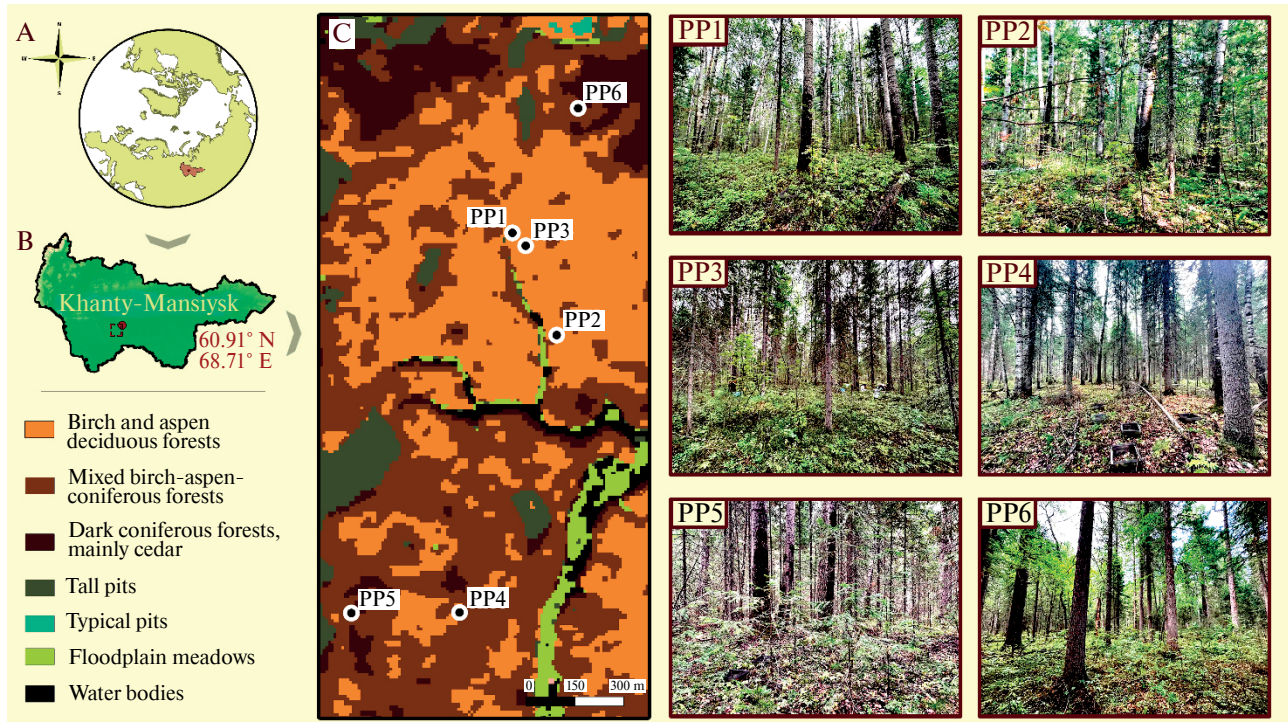


Fig. 1: Location of the studied sample areas: (a) in the Northern Hemisphere, (b) in Khanty-Mansi Autonomous Okrug-Yugra, (c) on the territory of the Mukhrino station. The map of the main types of ecosystems is based on classification with Sentinel-2 median image training for the periods from July 1 to August 15, 2021 and 2022. Photos of sample areas are presented on the right.

aspen forest (PP 1), passing into aspen forest with dark coniferous regeneration (PP 2), then into aspen forest with dark coniferous second story (PP 3), mixed dark coniferous-aspen forest (PP 4), dark coniferous forest with single large aspen trees (PP 5) and close to climax cedar forest (PP 6). Their detailed description is given below.

PP 1: bilberry-green-moss aspen forest. Total stand composition: 10P (common aspen (*Populus tremula* L.)). The average crown cover of the tree stand is 60 %, the height of the trees of the upper understorey is 20–22 meters. Rare specimens of cedar (*Pinus sibirica* Du Tour) and fir (*Abies sibirica* Ledeb.) with a height of 10–12 m and a crown cover of 0.5 % are present under the canopy of 50–60 years old aspen. Understory (5–10 %) is formed by Siberian mountain ash (*Sorbus aucuparia* subsp. *Sibirica* (Hedl.) Krylov), needle-leaved rosehip (*Rosa acicularis* Lindl.) and common wolfberry (*Daphne mezereum* L.). The herbaceous-shrub layer (50–60 %) is dominated by bilberry (*Vaccinium myrtillus* L.), bilberry (*Rubus saxatilis* L.) and cowberry (*Vaccinium vitis-idaea* L.). The area coverage of mosses is 20–30 %, among which *Hylocomium splendens* (*Hylocomium splendens* (Hedw.) Schimp.) predominates.

PP 2: small herb-green-moss aspen forest with dark coniferous regeneration. Total stand composition: 9P1C+B+F. The upper understorey (10P+B+F) is dominated by 60–80 years old aspen with a single admixture of birch (*Betula pubescens* Ehrh.) and fir. The average crown cover is 65 %, the average height of the upper tree layer is 22 m. The second

understorey (15–20 %) is formed by cedar young trees 2–8 (10) m high with insignificant admixture of spruce (9C1S). Understory (5–10 %) is formed by Siberian mountain ash, common bird cherry (*Prunus padus* L.), needle-leaved rosehip and common wolfberry. The herbaceous-shrub layer (50–60 %) is dominated by *Gymnocarpium dryopteris* (L.) Newman, bark bush and *Stellaria bungeana* Fenzl. The area cover of the moss layer is 50 %, dominated by *Rhytidadelphus triquetrus* (Hedw.) Warnst.

PP 3: bilberry-small-grass aspen forest with dark coniferous second understorey. Total stand composition: 6P2S1C1F+B. The average projective cover of the stand is 85 %. The upper tree layer is formed by aspen (10P), average tree height — 22 m, age — 80–100 years. The second understorey (crown cover — 20 %, height — 10–15 m) is dominated by spruce (*Picea obovata* Ledeb.) with participation of cedar and fir (5S3C2F+B). Understory (2–3 %) is formed by Siberian mountain ash, needle-leaved rosehip and common wolfberry. The herbaceous-shrub layer (70–80 %) is dominated by bilberry, common holocuttleberry and common sagebrush (*Oxalis acetosella* L.). The area cover of the moss layer is 20 %, dominated by shiny hylocomium.

PP 4: mixed small-grass-green-moss dark coniferous-aspen forest. Total stand composition: 3P2C2F2S1B. Its average cover is 90 %. The upper tree layer (60–70 %, composition 7P2B1S) is 25–29 m high, the age of aspen is 100–110 years. The lower tree layer (40 %, composition 6F2C1S1B) is 20 m high, coniferous species are 120–130 years old.

Understory (1–2 %) is formed by Siberian mountain ash and needle-leaved rosehip. The herbaceous-shrub layer (50–60 %) is dominated by *Maianthemum bifolium* (L.) F. W. Schmidt), common sagebrush and common hollyhock. The area cover of the moss layer is 30–40 %, dominated by shiny hylocomium.

PP 5: small herb-green-moss dark coniferous forest with single large aspen trees. Stand formula: 3C3S2F1P1B. Average coverage of the tree stand is 90 %. Crown cover of the upper tree layer (3P2C2S2B1F) — 50 %, of the lower tree layer (6F2S1C1B) — 60 %. Tree heights are 25–28 m and 12–15 m, respectively. The age of aspen in the forest layer is 100–120 years, cedar and spruce — 130–150 years. The understory (1 %) is formed by Siberian mountain ash and spikenard. The herbaceous-shrub layer is dominated by common hollyhock, Siberian dwarf (*Atragene sibirica* L.) and common sagebrush. Area cover of the herbaceous understorey is 0–10 % (dead-forest). Area cover of the moss layer — 5–10 %, dominated by *Hylocomium brilliantum* and *Rhytidadelphus triangularis*.

PP 6: cedar-small grass dark coniferous forest. Total stand composition: 8C2B+F with crown cover of 70–80 %. Average height of trees is 23–25 m, age of cedar — 130–150 years. Understory (10–20 % area cover) is formed by Siberian mountain ash (15 %) and spikenard (2–3 %). The herbaceous-shrub layer (50–60 %) is dominated by common holocuttleberry, bilberry and bony bush. The area cover of the moss layer is 60–70 %, dominated by shiny hylocomium.

Two organic sub-horizons are distinguished in all sample plots: Litter horizon L with an average thickness of up to 4 cm (in August), consisting of weakly decomposed compacted litter that retained its morphological features, well separated from the underlying one, and fermentative horizon F with a thickness of up to 6 cm, consisting of strongly decomposed compacted litter, poorly identifiable by morphological features, penetrated by mycelium, live and dead roots, and poorly separated from the underlying mineral horizon. According to L. G. Bogatyrev (1990), the studied litter is classified as fermentative weakly identified subprimitive low-moss coniferous-deciduous (PP 1–5) or deciduous-coniferous (PP6). Soils on the studied PPs are represented by light soils of illuvial-iron clay-illuviated unsaturated surface-light light-medium loam on alluvial deposits. Soil pH is acidic, increasing from 4.2–4.6 in the Eh horizon to 4.8–5.8 in the C horizon. Podzol horizon E in all PPs is discontinuous, irregular, not more than 10 cm thick. Climate, relief, vegetation and soils of the territory are described in detail in I. V. Kuprianova et al. Kuprianova et al. (2022).

Sampling. L-horizon litter was completely collected before leaf fall (August 27–28, 2023) and immediately thereafter (October 5–7, 2023) at six random 10×10 cm points in each sample area. L-horizon height was measured with a ruler at 24 random points in each PP. We proceeded from the assumption that fall composition reproduces from year

to year, and the L-horizon material collected in October can be considered as the initial substrate for decomposition, while that collected earlier in August — as the final phase before the arrival of fresh fall. Such an assumption is applicable for deciduous species, as well as cedar and fir, which fall most actively in the fall (Ivanov et al., 2018; Ivanova, 2021), but is not fully justified for spruce, half of the annual fall from which arrives in the winter-spring period and only about a quarter in the fall (Kuznetsov, 2010; Ivanova, 2021). However, spruce was not the predominant species at any of the PPs, and its influence on the litter input can be neglected.

Litterfall was collected between two L-horizon litter samplings using 5 circular fall traps of 0.25 m² each, randomly placed in each sampling area to avoid possible influence of parcellar structure on the results. The collected fall was transported to the laboratory, air-dried, sorted into fractions (aspen, rowan leaves, cedar, fir, spruce needles, branches (for all species), other) and weighed to the nearest 0.01g.

Sample preparation and IR spectra acquisition. L-horizon samples collected at points in the same sample area were manually mixed in the laboratory within a day after collection. From the mixed sample, a 100–200 g litter sample was taken and dried in a HyperCOOL HC3055 cold trap (Hanil, South Korea) for 48 hours. Then the dried samples were ground in two stages: firstly using a beaker-type knife mill (LZM-1M, Russia), and then using a MM 400 vibrating ball mill (Retsch, Germany). Immediately before taking spectra, 2 mg of the ground sample was mixed with 200 mg of potassium bromide (Specac, USA) using a pestle in an agate mortar. The resulting mixture was placed in a 13 mm diameter mold and pressed using a manual hydraulic press (Karaltay Scientific Instruments, China) at a maximum pressure of 4 tons. For each sample area, three analytical replicates (tablets) were made from the mixed sample.

Infrared spectra were taken in transmission mode using an IR-8000 FTIR spectrometer (Siberian Analytical Systems, Russia) controlled by OMNIC9.11.727 program (Thermo Fisher Scientific, USA) immediately after receiving the next tablet. The spectrum was recorded in the range of 400 to 4000 cm⁻¹ with a resolution of 4 cm⁻¹ with water vapor and carbon dioxide suppression enabled. The result for each sample was obtained by averaging 40 scans taken within a minute. The spectrum of a pure potassium bromide tablet without the addition of the sample, pressed in a similar manner, was used as the background spectrum. The background spectrum was taken after analyzing three samples from the same sample area

Spectra processing. In the instrument software, the spectra were converted from transmittance units to optical density units. Then the following steps were performed sequentially using the *ir* package version 0.2.1 (Teickner, 2023) in the R v.4.3.2 environment:

1. We performed baseline subtraction from the spectra with the *ir_bc* function using the *rubberband* method.

2. We performed smoothing using the Savitsky-Golay method with the *ir_smooth* function by a 2nd degree polynomial over 13 neighboring points of the spectrum.

3. We interpolated the data in 1 cm^{-1} intervals using the *ir_interpolate* function.

4. We removed the edges of the spectrum using the *ir_clip* function to clean the rest of the spectrum (850 to 3650 cm^{-1}) of edge artifacts.

5. Normalized using the *ir_normalize* function so that the area under each spectrum was equal to one.

These steps are recommended to reduce the influence of methodological features of spectrum acquisition (different mass of the sample, different position of the sample material in the pellet) and nuances of instrument operation (different signal-to-noise ratio in different parts of the range) on the final result (Hodgkins et al., 2018)

We calculated the contributions of optical densities to the first two principal components (obtained by the principal component method) and related the position of litter spectra from sample areas in the principal component coordinate axes relative to each other (Soong et al., 2015; Hodgkins et al., 2018). The principal component method was implemented using the *pca* function in the MATLAB2022a environment (MathWorks, USA), and the mean value was subtracted from the optical density values for each PP before calculations were performed. To allow a direct comparison of the contribution values of the optical densities at different wave numbers to both principal components at once, they were scaled into Z-counts according to their eigenvalues, as described in P. Legendre, L. Legendre (2012). The identification of functional groups characteristic of the fall and litter was performed using the wave numbers on which the peaks of the principal component contributions were found,

referring to the works of K. K. Pandey, A. J. Pitman (2003), J. Grabska et al. (2021), D. S. Volkov et al. (2021).

Elemental analysis. Total organic carbon and nitrogen contents were determined on an ECS8020 elemental analyzer (NC Technologies, Italy) by high-temperature combustion in excess oxygen (Dumas method) in the same samples used for spectra acquisition. A linear calibration was obtained by analyzing an alfalfa standard (Elemental Microanalysis, UK) with C = 42.35 % and N = 2.91 % in the mass range of 0.4 to 4 mg. Each sample was analyzed in three replicates at a 3 mg sample mass. The standard deviation for the same sample standard was $\pm 0.06\%$, $\pm 0.02\%$ and ± 0.2 for C, N and C/N respectively.

Stand age. The age of trees was determined by the number of annual rings at the uppermost root. It was determined by cores extracted from the trunk with a Haglof age drill (Sweden). In this case, the number of annual rings determined from the core was added to the number of years required for the tree to reach the sample height (20–25 cm height). For the predominant species, the age was determined for 3–5 typical trees, and for associated trees — for 1–3 typical trees.

Statistical processing. The results were analyzed in MATLAB2022a program (MathWorks, USA): one-factor analysis of variance — using the *anova1* function, multiple comparison — using the *multcompare* function based on Tukey's correction. The value of 0.05 was used as the threshold value of the confidence level.

RESULTS AND DISCUSSION

The total amount of the litterfall collected during the period August 27–28 to October 5–7 differed among sample plots ($p = 0.028$ for analysis of variance, $N = 30$). In general, it decreased from PP 1 ($273 \pm 28 \text{ g m}^{-2}$) to PP 6 ($167 \pm 24 \text{ g m}^{-2}$); values at these two PPs were the only ones that differed significantly in multiple comparisons

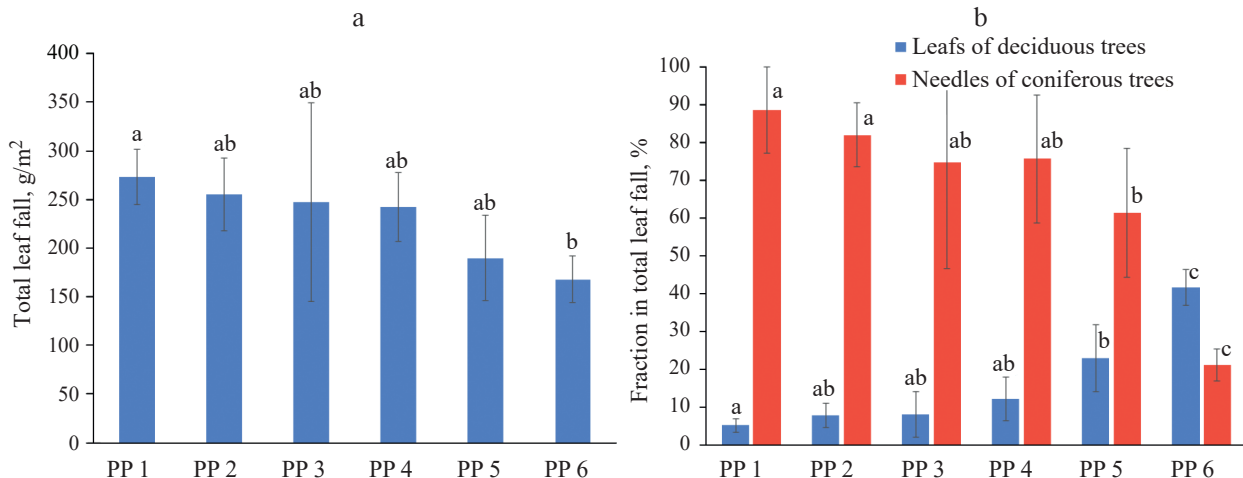


Fig. 2. (a) Total fall in the studied sample plots for the period August 27–28 — October 5–7, 2023; (b) proportion of small-leaved leaves and dark conifer needles in the fall in the studied sample plots. Letters denote differences in multiple comparisons: if any two bars have the same letter above them, the values in these bars are not significantly different.

(Fig. 2, a). The proportion of leaves of small-leaved species (aspen, mountain ash) in total fall was significantly different between sampling sites ($p < 0.0001$ for analysis of variance, $N = 30$): it decreased from PP 1 to PP 6, for which it was significantly lower in multiple comparisons than for the other PPs (Fig. 2, b). The proportion of dark coniferous fall (cedar, spruce and fir needles) was also significantly different between PPs ($p < 0.0001$ for analysis of variance, $N = 30$): it increased from PP 1 to PP 6, for which it was, on the contrary, significantly higher in multiple comparisons with the other PPs (Fig. 2, b). Mean L-horizon thickness differed significantly between PPs in August ($p = 0.0182$ for analysis of variance, $N = 24$), ranging from 2 to 4 cm. The only significant difference was between PP 2 (lowest value) and PP 4 (highest value). In October, the mean L-horizon thickness increased to 2.5–6 cm and also differed significantly between PPs ($p = 0.0014$ for analysis of variance, $N = 24$): for PP 1 and PP 3 the thickness was significantly higher than for PP 5 and PP 6.

L-horizon carbon content did not change significantly between PPs from October to August ($p = 0.42$ for analysis of variance, $N = 18$), ranging from 44 to 50 % (Table). The C/N ratio in the L-horizon decreased from October to August for all PPs (Table), with the magnitude of the change in C/N between these months differing significantly between PPs ($p < 0.0001$ for analysis of variance, $N = 18$). The largest decrease in C/N was observed for PP 5 and the smallest for PP 3; at the remaining PPs, the values of C/N change were intermediate between PP 5 and PP 3 and were not significantly different from each other in multiple comparisons (Fig. 3, a). In contrast, the total N content in the organic matter of the L-horizon increased from October to August. The magnitude of change in this content was also significantly different between PPs ($p < 0.001$ for analysis of variance, $N = 18$), the differences between PPs were the same as for C/N: total N increased most for PP 5, least for PP 3, and for the remaining PPs the changes in total N had intermediate values between PP 5 and PP 3 and were not significantly different from each other in multiple comparisons (Fig. 3, b).

The averaged IR spectra for samples from each sample area collected in August and October are shown in Fig. 4.

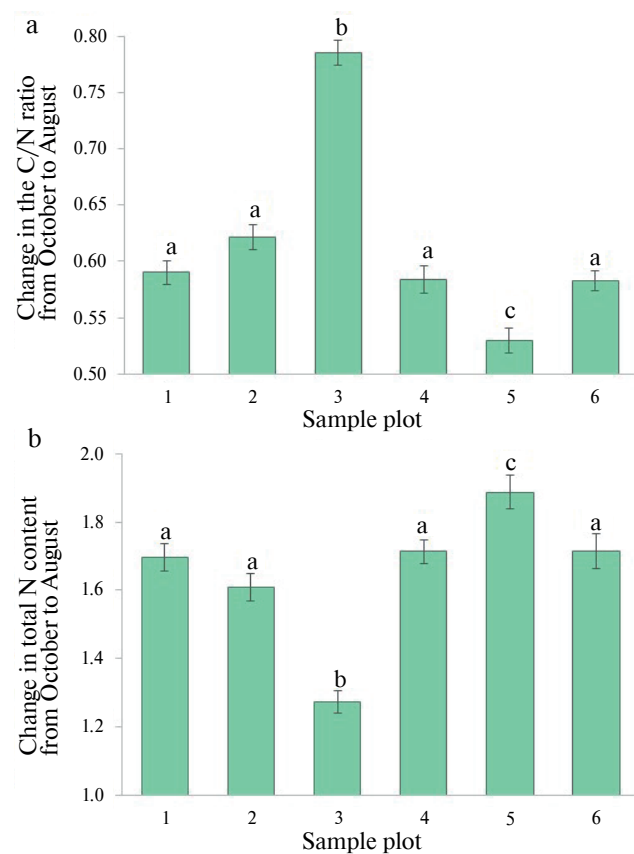


Fig. 3. (a) Decrease in C/N ratio in August relative to October for the studied L-horizon samples; (b) increase in N content in August relative to October for the studied L-horizon samples. Whiskers indicate standard deviation, letters indicate differences in multiple comparisons: if any two bars have the same letter above them, the values in those bars are not significantly different.

Principal component analysis of these spectra showed that in October the chemical structure of organic matter of the L-horizon litter gradually changed as the proportion of dark coniferous species increased from PP 1 to PP 5 (Fig. 5, a, circles), but had a fundamentally different composition at PP 6. Cellulose and other carbohydrates with peaks at wave numbers 1000–1100 cm^{-1} made comparable positive contributions to both principal components (Fig. 5, b). The first

Table. Dynamics of total C, N and C/N content in litter organic matter from October (highest proportion of fresh litter) to August (highest proportion of decomposed litter)

Sample area (PP)	Total C, %		Total N, %		C/N	
	October	August	October	August	October	August
1	45.1 (0.3)	44.8 (0.3)	1.06 (0.02)	1.80 (0.03)	42.4 (0.4)	25.0 (0.2)
2	46.0 (0.3)	45.8 (0.4)	0.86 (0.02)	1.39 (0.02)	53.3 (0.3)	33.1 (0.4)
3	46.5 (0.5)	45.9 (0.3)	1.14 (0.02)	1.46 (0.03)	40.7 (0.2)	31.9 (0.3)
4	49.1 (0.2)	49.3 (0.4)	1.02 (0.02)	1.74 (0.02)	48.3 (0.3)	28.2 (0.4)
5	49.2 (0.3)	49.1 (0.3)	1.02 (0.03)	1.93 (0.02)	48.1 (0.3)	25.5 (0.4)
6	47.4 (0.4)	47.2 (0.5)	0.85 (0.02)	1.46 (0.03)	55.5 (0.3)	32.3 (0.3)

Note. The mean (standard deviation) of three analytical replicates is given.

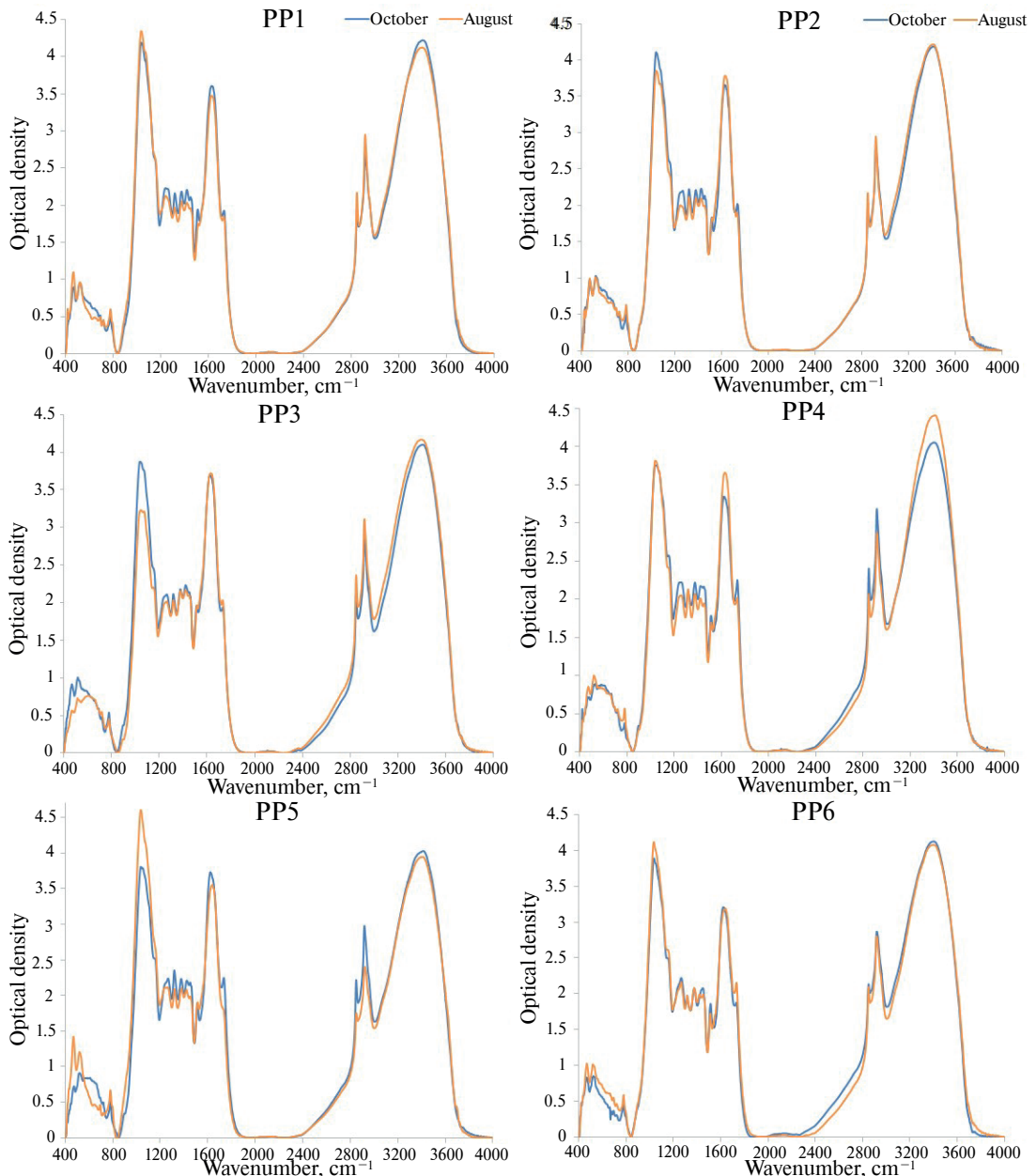


Fig. 4: Averaged IR spectra of samples from the L-horizon of the studied PPs. The averaged spectrum for the sample taken in October (after the leaf fall) is given in blue, while the orange spectrum is for the sample taken in August (the most decomposed litter).

principal component, explaining 55.2 % of the total variance, is also positively contributed by several peaks corresponding to proteins and other organic compounds with nitrogen: amide I (peak at 1650 cm^{-1}), amide II (1497 and 1565 cm^{-1}), and amide III (1235, 1326, and 1415 cm^{-1}). The peaks of aliphatic alkyl groups (C-H bonds at 2850 and 2918 cm^{-1}), carbonyl groups (C=O at 1738 cm^{-1}) and aromatic fragments (C=C, C=O and COOH in aromatic structures at 1617 cm^{-1}) contribute negatively to the second principal component (21.5 % of the dispersion). Thus, the more to the right of the point on the horizontal axis, the greater the proportion of nitrogen-containing compounds

in the litter, and the higher on the vertical axis, the smaller the proportion of recalcitrant aromatic compounds, polyesters (cutin, suberin, etc.) and lignin. The highest proportion of cellulose and carbohydrates is contained in the L-horizons of those PPs, samples from which are closer to the upper right corner.

In August, the pattern changed fundamentally (Fig. 5, a, squares): organic matter in L-horizons of the most contrasting objects — aspen (PP 1) and cedar (PP 6) — had similar characteristics, while aspen forests (PP 1, PP 2 and PP 3) and dark coniferous forests with insignificant participation of deciduous species (PP 5 and PP 6), which are at close

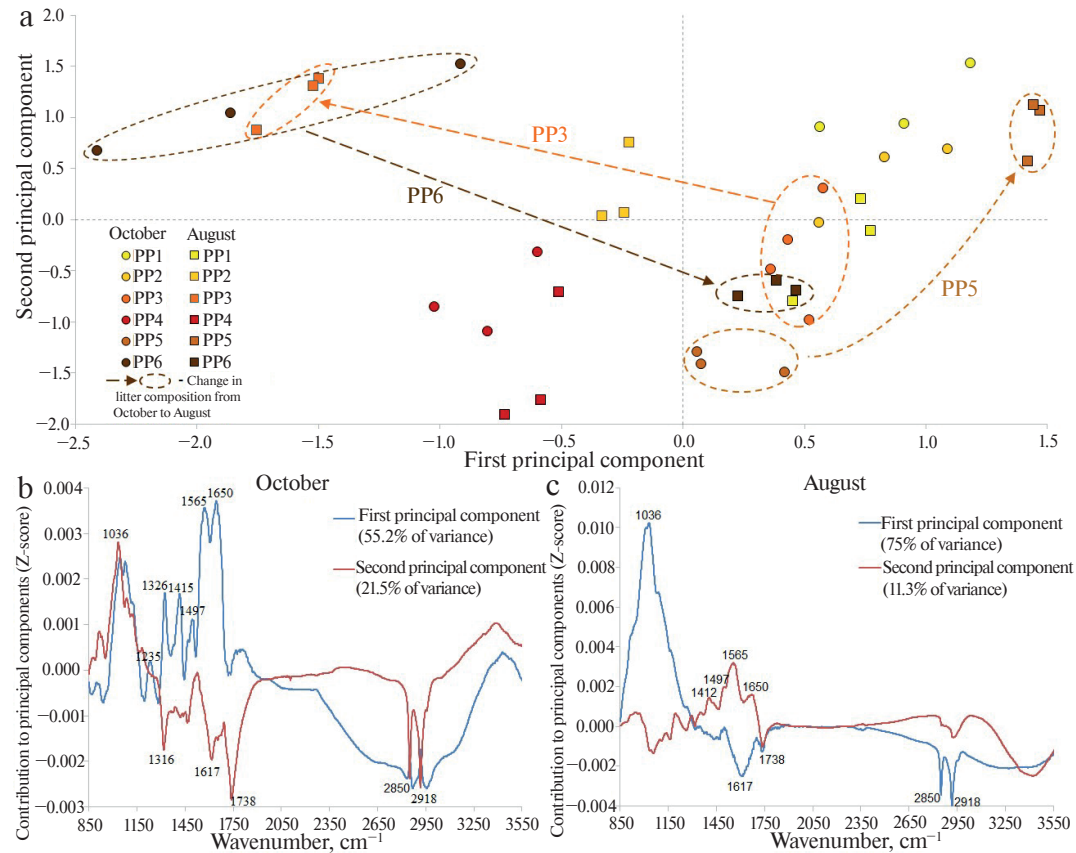


Fig. 5. (a) Position of the spectral characteristics in the principal component axes for the forest floor samples collected in October (circles) and August (squares) at the studied sample areas; (b, c) absorption contribution at different wave numbers to the first two principal components obtained by analyzing the spectra of L-horizons collected in October (b) and August (c) at the studied sample areas. The dotted arrows in plot (a) show the change in the position of the spectra of samples from the same sample area from October to August in the space of principal components. The numbers on the graphs (b, c) show the wave numbers at which the extrema of the largest peaks occur, for easy identification of the corresponding functional groups.

successional stages, began to differ significantly in the chemical structure of organic matter of L-horizons. At the same time, the same peaks contributed to the principal components, they were just differently distributed among the principal components (Fig. 5, c). The first principal component (75% of the variance) was positively contributed by cellulose and other carbohydrates (1000–1100 cm^{-1}) and negatively contributed by aromatic fragments (1617 cm^{-1}), carbonyl groups (1738 cm^{-1}), and aliphatic alkyl groups (2850 and 2918 cm^{-1}). The second principal component (11.3% of the dispersion) is positively contributed by proteins and other compounds with nitrogen (amide I–III) and negatively contributed by carbonyl groups (1738 cm^{-1}). Thus, the more to the right of the point on the horizontal axis, the greater the proportion of cellulose and carbohydrates and the smaller the proportion of recalcitrant aromatic compounds, and the higher on the vertical axis, the greater the proportion of nitrogen-containing compounds.

Differences in the composition of organic matter of the L-horizon litter sampled before and after leaf fall at different stages of secondary succession are formed for two reasons: due to the changing quality of incoming litter and due

to different litter transformation. The increasing proportion of conifers in the stand from PP 1 to PP 6 leads to a corresponding change in the structure of the fall, as observed in other studies (Ivanova, 2021). At the same time, only at PP 6 (near-climax dark coniferous forest) the fall was formed more by dark conifers than by small-leaved species. Although needle fall occurs year-round, this does not change the pattern we found, the proportion of dark coniferous fall will continue to increase in the same direction from PP 1 to PP 6. Analysis of IR spectra of the L-horizon of the forest floor in October (when it contains the most undecomposed litter) is fully consistent with the observed litterfall structure. The position of PP from 1 to 5 almost consistently decreases along the second principal component, which corresponds to a decrease in the proportion of easily degradable components (cellulose and carbohydrates) and accumulation of stable aromatics and polyesters. This is consistent with the well-known fact that dark coniferous species litterfall contains more recalcitrant compounds than deciduous litter (Artemkina, 2023; Berezin et al., 2023). The position of litter at PP 6 in the principal horizontal axes is fundamentally different from the other PPs: being located to the left of all PPs

along the abscissa axis, it contains significantly less proteins and other nitrogen-containing compounds.

As litter decomposes, the proportion of relatively easily degradable cellulose and carbohydrates in the litter falls and the proportion of stable components with a higher proportion of aromatic compounds increases (Cotrufo et al., 2009; Soong et al., 2015; Ivanova, 2021). The first principal component in August, which explains the vast majority of the variance in the spectra, accurately follows this trend, as the peak of cellulose and carbohydrates contributes positively to this principal component, while the peaks of lignin (1617 cm^{-1}) and polyesters (correlated peaks of carbonyl (1735 cm^{-1}) and aliphatic alkyl (2850 and 2918 cm^{-1}) groups) contribute negatively. In August, the proportion of cellulose and carbohydrates was lowest in the L-horizon sample PP 3, then increased in samples PP 2 and PP 4, then to PP 1 and PP 6, and was highest in sample from PP5. Comparison with the results for the L-horizon in October shows that the relative positions of several sample areas have changed (shown by arrows in Fig. 5, a). Samples from the L-horizon PP 2 and PP 3 lost the most cellulose and carbohydrates, moving these PPs significantly to the left of all others in August for the first principal component, although they had a higher proportion of these components in October than samples from PPs other than PP 1. Conversely, samples from the L-horizon PP 5 and PP 6 had less easily degradable components in October than the other PPs, and became more so in August. Samples from the L-horizon of aspen forest (PP 1), which in October exceeded samples from dark coniferous mature forest (PP 6) in cellulose fraction, became close to them by this indicator in August. Thus, the intensity of cellulose and carbohydrate decomposition decreased in the series $\text{PP 3} > 2 > 4 \approx 1 > 6 > 5$. In other words, the greatest relative decrease in the proportion of relatively easily decomposed cellulose and carbohydrates (and accumulation of recalcitrant components) occurred at the intermediate stages of succession, rather than at the initial stages, as previously assumed. Increased decomposition rates (and thus a greater decrease in the proportion of readily degradable substances in the same time) in mixed litter, compared to monospecific litter, have been repeatedly shown in litterbag experiments (Cotrufo, del Galdo, 2009; Yang et al., 2022). However, coniferous and deciduous litter falls on PPs 1–5 in comparable proportions, hence the effect of mixing of different litterfall types cannot explain the difference in organic matter transformation between these PPs. Another possible explanation could be related to element stoichiometry affecting organic matter transformation (Zechmeister-Boltenstern et al., 2015).

In terms of the change in the total nitrogen and C/N content in the L-horizon from October to August, PP 3 and PP 5 were at different poles, as well as in terms of the change in the chemical structure according to the FTIR spectrometry results. However, the conclusions derived from the elemental composition are opposite to the spectrometry results. The largest decrease in C/N (observed for PP 5) generally

corresponds to the most intense decomposition of the fallout, while the smallest decrease (observed for PP 3) corresponds to the least intense decomposition (Ge et al., 2013). This relationship has been attributed to overflow metabolism, where microorganisms, in order to access the nitrogen limiting their growth, spend resources on depolymerizing organic matter in the forest floor, reducing the efficiency of carbon assimilation (Zechmeister-Boltenstern et al., 2015). An alternative theory suggests that in nitrogen-poor ecosystems, preferential protein depolymerization controls nitrogen availability for microbes (Reuter et al., 2020). According to it, lower N accumulation and lower C/N increase during decomposition by PP 3 shows that microorganisms efficiently assimilate N from litter. If microorganisms have enough N, they can accumulate more biomass and decompose the litter more strongly, reducing the fraction of easily decomposable organic matter more than in other PPs. On the contrary, in the litter at PP 5, C/N decreased more strongly than at other PPs, that is, microorganisms are relatively less efficient in decomposing proteins, so the mass fraction of N in decomposing litter increased more than at other PPs. It can be assumed that under conditions of N deficiency microorganisms in litter on PP 5 are less active than on other PPs and provide less deep transformation of litter. Thus, the change in elemental composition during litter decomposition may be consistent with the conclusions obtained from FTIR spectrometry.

The accumulation of nitrogen compounds in the L-horizon at PP 5 from October to August is also confirmed by the results of FTIR spectrometry. However, the peaks in the range of 1200 – 1700 cm^{-1} at the first principal component in October and the second in August cannot be unambiguously interpreted as peaks of amide groups I–III, since absorption bands of other functional groups, including aromatic groups, exist in this region (Pandey and Pitman, 2003; Grabska et al., 2021; Volkov et al., 2021). The latter seems to be related to the fact that the spectra of L-horizon samples from PP 3 and PP 5 in August are close on the ordinate axis (second principal component), although the content of total nitrogen in them is very different. In addition, the shape of the principal components containing the peaks of amide groups I–III changes from October to August, for example, in August the peak at 1650 cm^{-1} became much lower than the peak at 1565 cm^{-1} compared to October, which also indicates that these principal components reflect not only the proportion of proteins in the organic matter of the L-horizon.

The analysis based on FTIR spectrometry has a several drawbacks. It does not allow us to determine quantitative differences in the accumulation of substances of a particular chemical structure in the L-horizon of different PPs. The increased proportion of polysaccharides for samples from PP 5 could be a consequence of the fact that spruce fall enters the L-horizon mainly in the winter-spring period and, as a consequence, it may be less decomposed in August compared to October. In addition, when mineral soil particles are mixed with litter samples, they may bias the results

because the absorption bands of aluminosilicates overlap with many organic matter absorption bands (Volkov et al., 2021). Nevertheless, the detected differences between the sample areas exceed the accuracy of the method, considering the scatter between the made replicates (symbols of the same color and shape in Fig. 5, a)

There are not many works in the literature that compare the rate or depth of fall transformation at intermediate and late stages of succession of upland middle taiga forest. Similar results were obtained by A. V. Ivanov (2015): in a mature (200 years) cedar-broadleaf forest, the litter-fall ratio, the inverse of the rate of fall decomposition, increases compared to the previous stages (50, 80, and 130 years), at which it is not significantly different. Incubation experiments with spruce litter, aspen litter and their mixture also confirm that the decomposition rate in litter depends not only on the composition of the litterfall but also on the composition of the stand forming that litter (Laganière et al., 2010). In this study, the mass loss (and hence the depth of transformation) of spruce needle fall increased during decomposition in aspen forest litter compared to spruce forest litter.

CONCLUSION

Litter decomposition plays a key role in the carbon and mineral nutrient cycles of forest ecosystems, especially in the boreal climate, where the lack of these mineral elements limits the productivity of phytocenoses and affects the rate of recovery after clearcuts and fires. Although decomposition rates at different stages of recovery successions have been measured many times, there are relatively few studies of changes in the chemical structure of litter during decomposition. We attempted to fill this gap using FTIR spectrometry, which combines the simplicity of implementation with the ability to compare the proportion of certain functional groups in the organic matter composition.

When fresh litter only enters the L-horizon, its chemical structure is determined primarily by the composition of this litter. Deciduous fall contains more easily degradable and less recalcitrant compounds, so in October the L-horizon of litter at later succession stages contains less of the former and more of the latter. The exception to this rule was litter in a near-climax dark coniferous forest, the L-horizon of which contained significantly less proteins than litter at earlier successional stages. If the decomposition of litter at different successional stages would depend solely on litter properties, the patterns obtained for L-horizon litter in October would have persisted (and probably intensified) by August. However, the analysis of IR spectra of L-horizons in August showed that the decomposition process itself at different stages of secondary succession proceeds differently and depends not only on the composition of the incoming litter. The strongest relative to other stages decrease in the share of easily decomposable and increase in the share of stable components occurred in the L-horizon of aspen forest with

dark coniferous second story, i. e. at the intermediate stage of succession among those studied. Closer to the initial and final stages, these changes decreased.

A possible explanation for this pattern can be derived from the elemental composition of decomposing litter, which directly controls the functioning of decomposers' communities. The increase in the total nitrogen content and decrease in C/N in the L-horizon were minimal exactly at the stage of succession where the strongest change in the chemical structure occurred. This may mean that microorganisms in this ecosystem extract nitrogen from litter more efficiently than at other stages. Since they most intensively decompose N-free, easily decomposable organic matter (cellulose and carbohydrates), the organic matter loses both C and N at the same time, resulting in a smaller change in the ratio of these elements in the L-horizon. At other succession stages, microorganisms are not that efficient in depolymerizing nitrogen-containing organic matter in the L-horizon, which results in a greater relative accumulation of nitrogen and, consequently, a greater decrease in C/N.

ACKNOWLEDGEMENTS

The research was carried out as part of the key innovative project of national importance "Key Innovative Project of National Importance, aimed to monitoring the dynamics of climatically active substances in terrestrial ecosystems of the Russian Federation" (Registration number: 123030300031-6).

REFERENCES

1. Adamczyk B., How do boreal forest soils store carbon?, *BioEssays*, 2021, Vol. 43, No. 7, p. 2100010. <https://doi.org/10.1002/bies.202100010>
2. Akkumulyatsiya ugleroda v lesnykh pochvakh i suktse-sionnyi status lesov (Carbon accumulation in forest soils and forest succession status), Moscow: Tovarishchestvo nauchnykh izdanii KMK, 2018, 232 p.
3. Angst G., Mueller K.E., Nierop K.G.J., Simpson M.J., Plant- or microbial-derived? A review on the molecular composition of stabilized soil organic matter, *Soil Biology and Biochemistry*, 2021, Vol. 156, p. 108189. <https://doi.org/10.1016/j.soilbio.2021.108189>
4. Artemkina N.A., Vzaimosvyazi fenol'nykh soedinenii, taninov, lignina, azota i ugleroda v rasteniyakh el'nikov kustarnichkovo-zelenomoshnykh na Kol'skom poluostrove (Physical-mechanical wood properties of pine culture of different planting density in Tambov region), *Lesovedenie*, 2023, No. 1, pp. 35–43. <https://doi.org/10.31857/S0024114823010047>
5. Basova E.V., Lukina N.V., Kuznetsova A.I. et al., Kachestvo drevesnogo opada kak informativnyi indikator funktsional'noi klassifikatsii lesov (Quality of wood litter as an informative indicator of functional classification

of forests), *Voprosy lesnoi nauki*, 2022, Vol. 5, No. 3, pp. 1–21.
<https://doi.org/10.31509/2658-607x-202252-113>

6. Berezin G.V., Kapitsa E.A., Shorokhova E.V., Sovremennye predstavleniya o razlozhenii drevesnogo opada v lesnykh ekosistemakh (Modern concepts of decomposition of wood litter in forest ecosystems), In: *Lesa Rossii: politika, promyshlennost', nauka, obrazovanie* (Forests of Russia: policy, industry, science, education). 2023, pp. 118–120.
7. Bogatyrev L.G., O klassifikatsii lesnykh podstilok (On forest litter classification), *Pochvovedenie*, 1990, No. 3, pp. 118–127.
8. Canadell J.G., Monteiro P.M.S., Costa M.H. et al., Syampungani S., Zaehle S., Zickfeld K., Global carbon and other biogeochemical cycles and feedbacks, *Climate change 2021: The physical science basis. Contribution of working group I to the sixth assessment report of the intergovernmental panel on climate change*, Cambridge University Press, 2021, pp. 673–816.
9. Cotrufo M.F., del Galdo I., Litter decomposition: concepts, methods and future perspectives, *Soil Carbon Dynamics*, 2009, pp. 76–90.
10. Cotrufo M.F., Galdo I.D., Piermatteo D., Litter decomposition: concepts, methods and future perspectives, *Soil Carbon Dynamics: An Integrated Methodology*, Cambridge: Cambridge University Press, 2010, pp. 76–90.
11. Fernández-Alonso M.J., Yuste J.C., Kitzler B., Ortiz C., Changes in litter chemistry associated with global change-driven forest succession resulted in time–decoupled responses of soil carbon and nitrogen cycles, *Soil Biology and Biochemistry*, 2018, Vol. 120, pp. 200–211.
<https://doi.org/10.1016/j.soilbio.2018.02.013>
12. Ge X., Zeng L., Xiao W. et al., Effect of litter substrate quality and soil nutrients on forest litter decomposition: A review, *Acta Ecologica Sinica*, 2013, Vol. 33, No. 2, pp. 102–108.
<https://doi.org/10.1016/j.chnaes.2013.01.006>
13. Grabska J., Beć K.B., Huck C.W., Current and future applications of IR and NIR spectroscopy in ecology, environmental studies, wildlife and plant investigations, *Comprehensive Analytical Chemistry*, 2021, Vol. 98, pp. 45–76.
<https://doi.org/10.1016/bs.coac.2020.08.002>
14. Heller C., Ellerbrock R.H., Roßkopf N., Klingensüß C., Zeitz J., Soil organic matter characterization of temperate peatland soil with FTIR-spectroscopy: effects of mire type and drainage intensity, *European J. of Soil Science*, 2015, Vol. 66, No. 5, pp. 847–858.
<https://doi.org/10.1111/ejss.12279>
15. Hodgkins S.B., Richardson C.J., Dommain R. et al., Tropical peatland carbon storage linked to global latitudinal trends in peat recalcitrance, *Nature Communications*, 2018, Vol. 9, No. 1, p. 3640.
<https://doi.org/10.1038/s41467-018-06050-2>
16. Ivanov A.V., Lynov D.V., Panfilova E.V., Braun M., Zamolodchikov D.G., Forest litters as a link in the carbon cycle in coniferous–broadleaved forests of the Southern Far East of Russia, *Eurasian Soil Science*, 2018, Vol. 51, No. 10, pp. 1164–1171.
17. Ivanov A.V., Zapasy lesnykh podstilok v ketrovo-shirokolistvennykh lesakh Yuzhnogo Sikhote-Alinya (Forest Litter Stocks in Korean Pine–Broad-Leaved Forests of the Southern Sikhote Alin), *Sibirskii lesnoi zhurnal*, 2015, No. 5, pp. 87–95.
<https://doi.org/10.15372/SJFS20150507>.
18. Ivanova E.A., Formirovaniye i razlozhenie drevesnogo opada v lesnykh ekosistemakh v fonovykh usloviyakh i pri aerotekhnogennom zagryaznenii (Tree litter production and decomposition in forest ecosystems under background conditions and industrial air pollution), *Voprosy lesnoi nauki*, 2021, Vol. 4, No. 3, pp. 1–52.
<https://doi.org/10.31509/2658-607x-202143-87>
19. Kharuk V.I., Ponomarev E.I., Ivanova G.A., Dvinskaya M.L., Coogan S.C.P., Flannigan M.D., Wildfires in the Siberian taiga, *Ambio*, 2021, Vol. 50, No. 11, pp. 1953–1974.
<https://doi.org/10.1007/s13280-020-01490-x>
20. Kobak K.I., *Bioticheskie komponenty uglerodnogo tsikla* (Biotic components of the carbon cycle), Leningrad: Gidrometeoizdat, 1988, 248 p.
21. Kupriianova I.V., Kaverin A.A., Filippov I.V. et al., The main physical and geographical characteristics of the Mukhrino field station area and its surroundings, *Environmental Dynamics and Global Climate Change*, 2022, Vol. 13, No. 4, pp. 215–252.
<https://doi.org/10.18822/edgcc240049>
22. Kuznetsov M.A., Vliyanie uslovii razlozheniya i sostava opada na kharakteristiki i zapas podstilki v srednetaezhnom chernichno-sfagnovom el'nike (Effect of decomposition conditions and falloff composition on litter reserves and characteristics in a bilberry-sphagnum spruce forest of middle taiga), *Lesovedenie*, 2010, No. 6, pp. 54–60.
23. Laganière J., Pare D., Bradley R.L., How does a tree species influence litter decomposition? Separating the relative contribution of litter quality, litter mixing, and forest floor conditions, *Canadian J. of Forest Research*, 2010, Vol. 40, No. 3, pp. 465–475.
24. Legendre P., Legendre L., Numerical ecology, *Developments in Environmental Modelling*, Vol. 24, Amsterdam: Elsevier Science BV, 2012, 989 p.
25. Lukina N.V., Global'nye vyzovy i lesnye ekosistemy (Global challenges and forest ecosystems), *Vestnik RAN*, 2020, Vol. 90, No. 6, pp. 528–532.
<https://doi.org/10.31857/S0869587320060080>
26. Pandey K.K., Pitman A.J., FTIR studies of the changes in wood chemistry following decay by brown–rot and white–rot fungi, *International Biodeterioration and Biodegradation*, 2003, Vol. 52, No. 3, pp. 151–160.
[https://doi.org/10.1016/S0964-8305\(03\)00052-0](https://doi.org/10.1016/S0964-8305(03)00052-0)
27. Práválie R., Major perturbations in the Earth's forest ecosystems. Possible implications for global warming, *Earth-Science Reviews*, 2018, Vol. 185, pp. 544–571.
<https://doi.org/10.1016/j.earscirev.2018.06.010>
28. Reuter H., Gensel J., Elvert M., Zak D., Evidence for preferential protein depolymerization in wetland soils in response to external nitrogen availability provided by a novel FTIR routine, *Biogeosciences*, 2020, Vol. 17, No. 2, pp. 499–514.
<https://doi.org/10.5194/bg-17-499-2020>

29. Semenov V.M., Tulina A.S., Semenova N.A., Ivannikova L.A., Humification and nonhumification pathways of the organic matter stabilization in soil: A review, *Eurasian Soil Science*, 2013, Vol. 46, No. 4, pp. 355–368.

30. Soong J.L., Parton W.J., Calderon F., Campbell E.E., Cotrufo M.F., A new conceptual model on the fate and controls of fresh and pyrolyzed plant litter decomposition, *Biogeochemistry*, 2015, Vol. 124, No. 1–3, pp. 27–44. <https://doi.org/10.1007/s10533-015-0079-2>

31. Volkov D.S., Rogova O.B., Proskurnin M.A., Organic matter and mineral composition of silicate soils: FTIR comparison study by photoacoustic, diffuse reflectance, and attenuated total reflection modalities, *Agronomy*, 2021, Vol. 11, No. 9, pp. 1879. <https://doi.org/10.3390/agronomy11091879>

32. Wardle D.A., Bardgett R.D., Klironomos J.N. et al., Ecological linkages between aboveground and belowground biota, *Science*, 2004, Vol. 304, No. 5677, pp. 1629–1633.

33. Yang K., Zhu J., Zhang W. et al., Litter decomposition and nutrient release from monospecific and mixed litters: Comparisons of litter quality, fauna and decomposition site effects, *J. of Ecology*, 2022, Vol. 110, No. 7, pp. 1673–1686. <https://doi.org/10.1111/1365-2745.13902>

34. Zechmeister-Boltenstern S., Keiblinger K.M., Mooshamer M. et al., The application of ecological stoichiometry to plant–microbial–soil organic matter transformations, *Ecological Monographs*, 2015, Vol. 85, No. 2, pp. 133–155. <https://doi.org/10.1890/14-0777.1>

35. Zhang K., Cheng X., Dang H. et al., Linking litter production, quality and decomposition to vegetation succession following agricultural abandonment, *Soil Biology and Biochemistry*, 2013, Vol. 57, pp. 803–813. <https://doi.org/10.1016/j.soilbio.2012.08.005>